International Journal of Computer Information Systems and Industrial Management Applications
ISSN 2150-7988 Volume 18(22s) 2026 pp. 492-514
https://doi.org/10.70917/ijcisim-2026-5456
Article

A Multimodal Biosignal Fusion Framework for Epileptic Seizure Detection Using Machine Learning, Ensemble Learning, and Optimization

Abdul-Mumin Khalid*[1], Musah Sulemana[2], Wahab Abdul Iddrisu[3]

[1]Department of Mathematics and ICT, E.P. College of Education, Bimbilla. Ghana
[2]Department of Mathematics, University for Development Studies, Tamale. Ghana
[3]Department of Mathematics & Statistics, Ghana Communication Technology University, Ghana

Abstract: Epileptic seizure detection requires reliable analysis of complex physiological changes that may not be adequately represented by a single biosignal. This study developed an optimized multimodal biosignal fusion framework integrating electroencephalography (EEG), electrocardiography (ECG), electromyography (EMG), and accelerometer (ACC) signals for automated seizure detection. Data from 120 patients were processed using data quality assurance, preprocessing, feature extraction, and patient-wise partitioning to minimize data leakage. A parameterized quadratic fusion framework was applied to capture complementary and nonlinear cross-modal interactions and evaluated using twelve traditional machine-learning and deep-learning models. Particle Swarm Optimization (PSO) was employed for joint optimization of model and fusion parameters, while SHAP and PCA supported model interpretation. In addition, ensemble-learning strategies were tested for robustness and generalizability. Full quasi-quadratic fusion achieved 98.10% accuracy, 97.40% F1-score, and 98.90% AUC, while full EEG–ECG–EMG–ACC fusion achieved 99.67% accuracy and 99.79% AUC. The smallest generalization gap (ΔAUC = 0.60 percentage points) was also obtained from the fusion-aware ensemble. In summary, the results presented here demonstrate that fundamental techniques of quadratic multimodal fusion and optimization methods in machine learning for explainable ensemble approaches, when applied together, can afford an accurate, interpretable, and well-generalized fail-safe framework for multimodal automated epileptic seizure detection.

Keywords: Epileptic seizure detection; Multimodal biosignal fusion; EEG; ECG; EMG; Accelerometer; Particle Swarm Optimization; Machine learning; Deep learning; Ensemble learning

1. Introduction

Epilepsy is a major neurological disorder characterized by recurrent seizures resulting from abnormal electrical activity in the brain. It affects millions of people worldwide and remains particularly challenging in low- and middle-income countries, where access to continuous neurological monitoring and specialized diagnostic services may be limited (Adamu et al., 2023). Accurate and timely detection of epileptic seizures is therefore important for diagnosis, patient monitoring, treatment support, and the development of automated seizure-detection systems.

Electroencephalography (EEG) remains the principal physiological signal used for seizure detection because it directly reflects electrical activity in the brain. However, seizure events can also produce changes in cardiac activity, muscle contractions, and body movement that can be captured through electrocardiography (ECG), electromyography (EMG), and accelerometer (ACC) signals. Reliance on EEG alone may therefore overlook complementary physiological information associated with seizure activity. Furthermore, EEG recordings may be affected by noise, artifacts, patient variability, and recording conditions, which can influence the reliability of automated seizure-detection systems (Li et al., 2022; Zhang et al., 2024).

Multimodal biosignal fusion provides an opportunity to address some of these limitations by combining information from different physiological sources. Integrating EEG, ECG, EMG, and ACC signals can provide complementary representations of the neural, cardiac, muscular, and movement-related manifestations of seizures (Fan et al., 2026). Nevertheless, existing multimodal approaches often use only a subset of these modalities or employ relatively simple fusion techniques. Consequently, the higher-order interactions and complementary relationships among multiple biosignals may not be adequately represented (Zhang et al., 2024; Fan et al., 2026).

Machine-learning and deep-learning methods have increasingly been applied to automatic seizure detection. Traditional algorithms such as Support Vector Machine (SVM), Random Forest (RF), Decision Tree (DT), K-Nearest Neighbour (KNN), Logistic Regression (LR), and XGBoost provide useful classification mechanisms, while deep-learning architectures such as Convolutional Neural Networks (CNN), Long Short-Term Memory (LSTM), Gated Recurrent Unit (GRU), Temporal Convolutional Network (TCN), Transformer, and CNN–LSTM can capture more complex temporal and nonlinear patterns in physiological signals. However, previous studies commonly evaluate only a limited number of models, making it difficult to determine whether improvements obtained from a particular fusion strategy are consistent across heterogeneous model families (Naser, 2026; Mourad et al., 2025).

Another challenge concerns model optimization. The performance of machine-learning and deep-learning models depends considerably on appropriate hyperparameter selection and the configuration of the fusion mechanism. Conventional manual or exhaustive tuning procedures may become inefficient when several models, modalities, and fusion parameters are considered simultaneously. Particle Swarm Optimization (PSO) provides a population-based optimization mechanism capable of exploring complex parameter spaces while balancing exploration and exploitation (Li et al., 2024). Its integration with multimodal seizure detection therefore provides an opportunity to jointly optimize model hyperparameters and parameters controlling interactions among different biosignal modalities.

Interpretability and generalizability are equally important for clinically oriented seizure-detection systems. Although deep-learning models can achieve high classification performance, their complex decision processes may be difficult to interpret. Explainable artificial intelligence techniques such as SHapley Additive exPlanations (SHAP) can quantify the contributions of individual features and modalities to model predictions, while Principal Component Analysis (PCA) can provide lower-dimensional visualization of seizure and non-seizure patterns. However, the integration of explainability techniques within optimized multimodal and ensemble seizure-detection frameworks remains relatively limited (Zhou et al., 2025).

Ensemble learning provides another mechanism for improving prediction stability and robustness by combining the outputs of multiple models. Approaches such as bagging, boosting, stacking, and majority voting can exploit complementary characteristics of heterogeneous learners and reduce dependence on the weaknesses of individual models (Mohammed & Kora, 2023; Rane et al., 2024). Despite advances in multimodal fusion, optimization, explainability, and ensemble learning, these components are frequently investigated independently rather than within a unified seizure-detection framework (Fang et al., 2025; Zhang et al., 2022).

Therefore, this study presents an integrated and optimized multimodal biosignal fusion framework for epileptic seizure detection using EEG, ECG, EMG, and ACC signals. The framework incorporates data quality assurance and preprocessing, a parameterized quadratic multimodal fusion representation, twelve traditional machine-learning and deep-learning models, SHAP- and PCA-based interpretation, Particle Swarm Optimization, and ensemble-learning strategies. The fusion framework is systematically evaluated across individual, pairwise, tri-modal, and complete four-modal configurations, while patient-wise data partitioning and cross-dataset evaluation are employed to assess generalizability.

The principal contribution of this study is the integration of these components into a single end-to-end framework capable of modelling complementary and nonlinear interactions among multiple physiological signals while simultaneously addressing optimization, interpretability, robustness, and generalization. The study consequently provides a comprehensive assessment of how multimodal interaction modelling, heterogeneous learning architectures,

optimization, explainability, and ensemble learning can jointly contribute to reliable automated epileptic seizure detection.

2. Literature Review

2.1 Machine Learning and Deep Learning for Seizure Detection

Machine-learning techniques have become important tools for identifying discriminative patterns in physiological signals and distinguishing seizure from non-seizure activity (Akrami et al., 2024). Traditional machine-learning approaches generally rely on extracted features and offer relatively interpretable classification mechanisms. Algorithms such as Random Forest (RF), Support Vector Machine (SVM), K-Nearest Neighbour (KNN), Decision Tree (DT), Logistic Regression (LR), and XGBoost have consequently been applied to biomedical classification problems (Ghosh et al., 2024; Chen et al., 2024).

Deep-learning models provide greater capacity for learning complex temporal and nonlinear relationships directly from biosignal representations. CNNs are effective for extracting spatial and temporal patterns, while recurrent architectures such as LSTM and GRU capture temporal dependencies in sequential physiological data (Cockburn et al., 2022; Hussein & Al Jumaily, 2025; Adamu et al., 2023). TCNs provide temporal modelling through dilated causal convolutions, whereas Transformers use attention mechanisms to capture long-range relationships among sequential features (Bai et al., 2026; Li et al., 2025). CNN–LSTM architectures further combine feature extraction with temporal modelling (Roy & Lolam, 2025). However, many existing studies evaluate only a limited number of model architectures, restricting broad comparison across heterogeneous machine-learning and deep-learning families (Naser, 2026; Mourad et al., 2025).

2.2 Multimodal Biosignal Fusion

Multimodal fusion combines complementary information from different physiological signals to provide a more comprehensive representation for classification. In seizure detection, EEG represents neurological activity, while ECG, EMG, and ACC provide complementary information related to cardiac activity, muscular responses, and body movement. Combining these signals can therefore improve robustness compared with relying on a single modality, particularly when individual signals are affected by noise or artifacts (Saleh et al., 2025).

Existing fusion methods can operate at feature, decision, or model levels, depending on how information from different modalities is combined (Ahmad et al., 2026; Zhang et al., 2024). However, EEG remains dominant in seizure-detection research, and relatively few studies simultaneously integrate EEG, ECG, EMG, and ACC (Fan et al., 2026). This creates a need for fusion approaches capable of explicitly representing complementary and higher-order interactions among multiple biosignal modalities.

2.3 Particle Swarm Optimization

The performance of machine-learning and deep-learning models depends strongly on appropriate parameter and hyperparameter selection. Particle Swarm Optimization (PSO) is a population-based optimization technique in which candidate solutions are iteratively updated according to individual and collective search experiences (Jie et al., 2025). Its ability to balance exploration and exploitation makes it useful for nonlinear and high-dimensional optimization problems (Wei et al., 2019).

Although optimization techniques have been applied to biomedical classification, the joint optimization of model hyperparameters and multimodal fusion parameters in seizure-detection systems remains comparatively limited (Bai et al., 2025). PSO therefore provides a suitable mechanism for optimizing both model configurations and parameters controlling multimodal interactions.

2.4 Explainability Using SHAP and PCA

Interpretability remains important for machine-learning applications involving clinical data, particularly as deep-learning architectures become increasingly complex (Zhou et al., 2025). SHapley Additive exPlanations (SHAP) provides a mechanism for quantifying the contribution of individual features and modalities to model predictions. Principal Component Analysis (PCA), in contrast, reduces high-dimensional feature representations and enables visualization of seizure and non-seizure patterns within the feature space.

A parameterized multimodal feature-fusion approach integrating PCA and SHAP has further demonstrated that explainability can be incorporated directly into multimodal seizure-detection frameworks to assess feature importance, modality contributions, and seizure/non-seizure class separability (Khalid et al., 2026)

The combined application of SHAP and PCA can therefore provide complementary perspectives on model interpretation: SHAP explains feature contributions, while PCA illustrates class-separation patterns. However, their integration within optimized multimodal seizure-detection frameworks remains relatively limited (Zhang et al., 2024; Zhou et al., 2025).

2.5 Ensemble Learning and Research Gap

Ensemble learning combines predictions from multiple models to improve classification accuracy, stability, and robustness. Common approaches include bagging, boosting, stacking, and majority voting. These strategies exploit complementary learning characteristics among base models and can reduce dependence on the weaknesses of individual classifiers (Mohammed & Kora, 2023; Rane et al., 2024).

Despite advances in seizure detection, important limitations remain. Existing studies frequently depend on EEG or limited multimodal combinations, evaluate relatively few learning architectures, employ separate optimization procedures, and provide limited integration of explainability and ensemble learning. More importantly, multimodal fusion, optimization, explainability, and ensemble learning are often investigated independently rather than as components of a unified seizure-detection framework (Fang et al., 2025; Zhang et al., 2022).

The present study addresses these limitations through an integrated framework that combines EEG, ECG, EMG, and ACC signals; employs quadratic multimodal fusion; includes 12 machine-learning and deep-learning models; uses PSO-based optimization; applies SHAP and PCA for interpretation; and employs ensemble learning within a common seizure-detection architecture.

3. Methodology

This study employed a quantitative experimental framework integrating multimodal biosignal preprocessing, quadratic fusion, twelve machine-learning and deep-learning models, SHAP/PCA interpretation, Particle Swarm Optimization (PSO), and ensemble learning for epileptic seizure detection. The methodology comprised data acquisition and quality assurance, patient-wise data partitioning, feature extraction, multimodal fusion, model development, optimization, interpretation, and generalizability assessment.

3.1 Dataset and Signal Acquisition

Table 1. Summary of Dataset and Signal Acquisition Characteristics

Item	Value
Total patients	120
Data sources	Tamale Teaching Hospital (TTH) + Public repository
Modalities	EEG, ECG, EMG, ACC
Sampling rate	512 Hz

Window length	2 seconds
Overlap	50%
Total segmented windows	≈ 1,024,000
Splitting protocol	Patient-wise split (to prevent data leakage)
Training set	70% (≈ 716,800 windows)
Validation set	15% (≈ 153,600 windows)
Test set	15% (≈ 153,600 windows)

3.2 Ethics Approval and Data Governance

Ethical approval and institutional permission were obtained for the use of the clinical data from Tamale Teaching Hospital (TTH). The hospital records used in the study were previously collected and anonymized before analysis, with no patient-identifiable information included in the research dataset. Publicly available datasets were accessed and used in accordance with their respective data-use requirements. All data were stored and processed securely and used solely for research purposes. The study involved retrospective analysis of existing biosignal data and did not involve direct intervention with patients.

3.3 Proof of Patient-Wise Data Splitting and Leakage Prevention

The 120 patients were partitioned into mutually exclusive training (70%), validation (15%), and testing (15%) subsets before model development. All signal windows generated from an individual patient were retained within the same partition, ensuring that no patient contributed observations to more than one dataset subset. This patient-wise procedure minimized subject-level information leakage and enabled evaluation on previously unseen patients.

where pN=120 represents the total number of patients. For each patient, let denote the complete set of segmented signal windows belonging to that patient. The complete dataset can therefore be expressed as:

$$\mathcal{D} = \bigcup_{i=1}^{120} \mathcal{W}_{p_i} \qquad (1).$$

The patients were divided into three mutually exclusive subsets: training, validation, and testing:

subject to:

$$\mathcal{P}_{train} \cap \mathcal{P}_{val} = \mathcal{P}_{train} \cap \mathcal{P}_{test} = \mathcal{P}_{val} \cap \mathcal{P}_{test} = \emptyset \qquad (3).$$

The corresponding signal windows were then assigned according to the patient subset:

$$\mathcal{D}_{train} = \bigcup_{p \in \mathcal{P}_{train}} \mathcal{W}_p \, , \mathcal{D}_{val} = \bigcup_{p \in \mathcal{P}_{val}} \mathcal{W}_p \, , \mathcal{D}_{test} = \bigcup_{p \in \mathcal{P}_{test}} \mathcal{W}_p \qquad (4).$$

3.4 Evaluation Metrics

For evaluating model performance, three primary metrics were employed: Accuracy, F1-score, and Area Under the Receiver Operating Characteristic Curve (AUC). These metrics were chosen to provide complementary evaluations of overall classification accuracy, balance between precision and recall, and discriminatory performance across classification thresholds.

Accuracy: the fraction of correctly classified seizure or non-seizure observations in total (i.e., among all Observations).

$$ACC = \frac{TP + TN}{TP + TN + FP + FN} \quad (5).$$

F1-Score

The F1-score denotes the harmonic mean of precision and recall and is particularly useful when evaluating classification presentation where class distributions may be imbalanced:

$$F1 - s = 2 \times \frac{Precision \times Recall}{Precisio + Recall} \quad (6).$$

where:

$$\text{Precision} = \frac{TP}{TP + FP} \quad (7).$$

And

$$Recall = \frac{TP}{TP + FN} \quad (8).$$

Area Under the ROC Curve (AUC)

AUC measures the ability of a classifier to distinguish between seizure and non-seizure classes across different decision thresholds. It is derived from the Receiver Operating Characteristic (ROC) curve, which plots the True Positive Rate (TPR) against the False Positive Rate (FPR):

$$TPR = \frac{TP}{TP + FN} \quad (9).$$

$$FPR = \frac{FP}{FP + TN} \quad (10).$$

The AUC can therefore be represented as:

$$AUC = \int_0^1 TPR(FPR)\, d(FPR) \quad (11).$$

The closer the AUC to 1, the more separation between observations with a seizure and those without.

Denotes the F1 score, which was used in this study as the main criterion, since it balances recall and precision, reducing dependence on accuracy. Overall classification accuracy was quantified, whereas the model's discriminative ability, a measure independent of any threshold, was assessed using AUC. These three metrics together were used to compare the baseline models, quadratic-modified models, PSO-optimized models' multimodal fusion setups and ensemble-learning strategies.

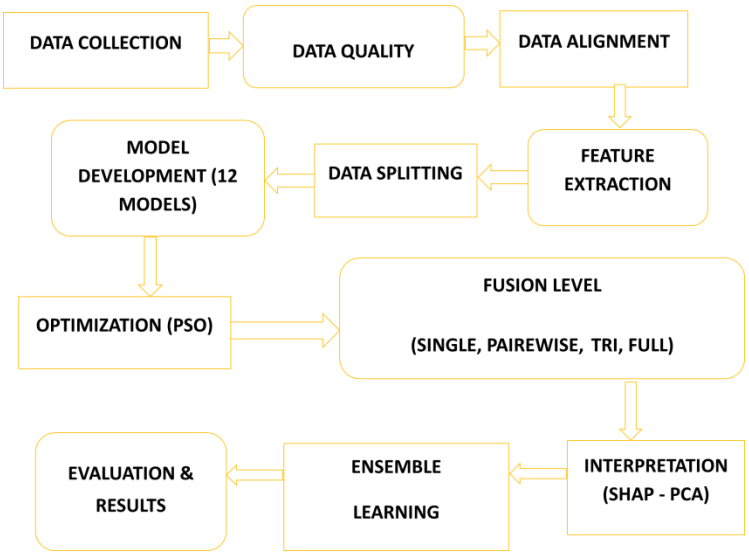

Figure 1. General workflow of the proposed seizure detection framework

3.5 Data Quality Assurance (DQA) Framework

In this study, a Similarity Score (S) was incorporated to quantify the degree of cross-modal agreement within each 2-second observation window. The score provides a standardized measure of correspondence among modality pairs and complements the modality-specific quality measures included in the Data Quality Assurance framework. Higher resemblance values show stronger agreement among synchronized modalities, while lower values indicate weaker correspondence that may arise from noise, artifacts, or modality-specific variability.

We applied a systematic Data Quality Assurance (DQA) framework to determine the reliability of every 2-sec window of EEG, ECG, EMG and ACC signals prior to feature extraction and model development. These quality dimensions, which are complementary to each other, were completeness (α),consistency (β) validity (γ), and cross-modal reliability (η). The last three served as standard metrics for signal-window quality, each ranging from 0 to 1, and were combined into a Data Quality Index (DQI).

The DQA framework aimed to detect and censor windows with large amounts of missing information, excessive signal fluctuations, obviously physiologically implausible values, or poor cross-modality consistency. Consequently, higher DQI values represented more highly reliable windows in which signals could be detected, while lower values signified noisy or unreliable observations.

$$DQA = \alpha C + \beta S + \gamma V \qquad (12).$$

Where:

α, β, γ are the weighting coefficients.

C: Completeness

S: Consistency

V: Validity (noise-to-signal)

Threshold: 0.85

The Data Quality Assurance equation is then defined as:

$$DQA_{m,s} = \alpha\left(\frac{N_{val}}{N_{exp}}\right) + \beta\left(\frac{\rho_{ms}}{\max(\rho_{ms})}\right) + \gamma\left(1 - \frac{Noise_{m,s}}{Signal_{m,s}}\right)^{\delta_m} \qquad (13).$$

$$DQA|_{Total} = \frac{1}{8}\sum_{m=1}^{4}\sum_{s=1}^{2} DQA_{m,s} \qquad (14).$$

Where:

$D_{(m,s)}$ Denote the dataset of modality, that is

$S \in TTH, Public$ Represent the source,

N_{exp} = expected number of data points (1,024,000),

N_{val} = number of valid points after preprocessing

ρ_{ms} = pairwise correlation (signal alignment across modalities)

δ_m = modality reliability factor (derived from noise and artifact removal efficiency)

α, β, λ = Tunable weighting parameters for completeness, consistency, and validity, respectively.

Quadratic fusion ensures that a single poor-quality component significantly lowers DQI, preventing noisy segments from passing.

$$0 \leq \text{DQI} \leq 1 \qquad (15).$$

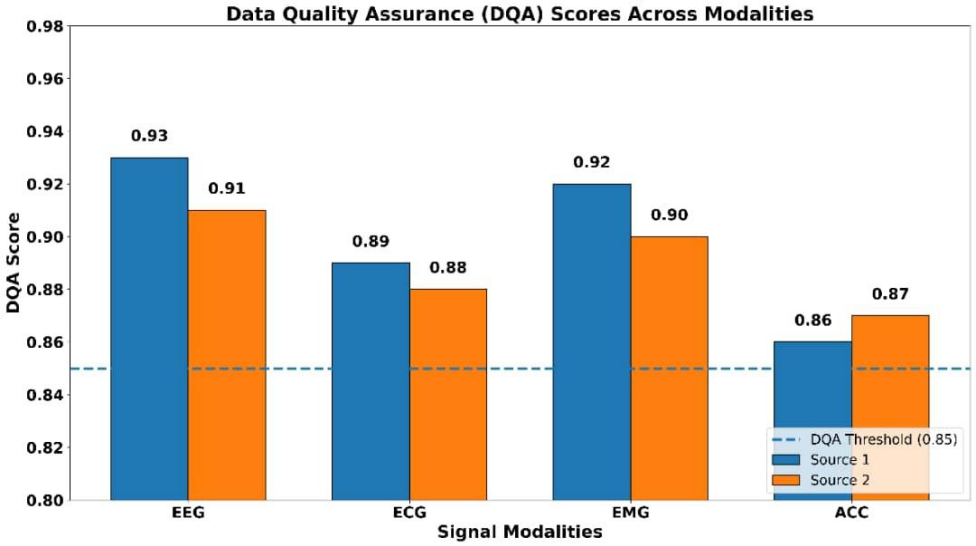

Figure 2. Data Quality and Alignment Framework

3.6 Preprocessing, Normalization and Feature Extraction

Following segmentation and Data Quality Assurance (DQA), the retained EEG, ECG, EMG, and ACC signal windows were preprocessed to reduce noise, artifacts, and signal inconsistencies. The processed signals were subsequently normalized to minimize scale differences across modalities and patients.

To reduce scale differences among EEG, ECG, EMG, and ACC features, min–max normalization was applied. For each feature, the minimum and maximum values were estimated from the training data and subsequently applied unchanged to the validation and patient-wise test sets. This procedure prevented information from the validation or test sets from influencing the normalization process.

$$x_{\text{norm}} = \frac{x - x_{\min}}{x_{\max} - x_{\min}} \qquad (16).$$

Where:

x: raw feature

$x_{\min}$, $x_{\max}$: minimum and maximum values in the window

x_{norm}: normalized feature within [0,1]

This step ensures all features from EEG, ECG, EMG, and ACC contribute equally in subsequent processing.

Following preprocessing and normalization, three descriptive features were extracted from each 2-second window of EEG, ECG, EMG, and ACC signals: **Entropy, Energy, and Root Mean Square (RMS)**.

A. Entropy-Based Features

$$H = -\sum_{i=1}^{n} p_i \log(p_i) \qquad (17).$$

B. Energy features and Signal Energy

$$E = \sum_{t=1}^{N} x(t)^2 \qquad (18).$$

C. Root Mean Square (RMS)

$$\text{RMS} = \sqrt{\frac{1}{N}\sum_{t=1}^{N} x(t)^2} \qquad (19).$$

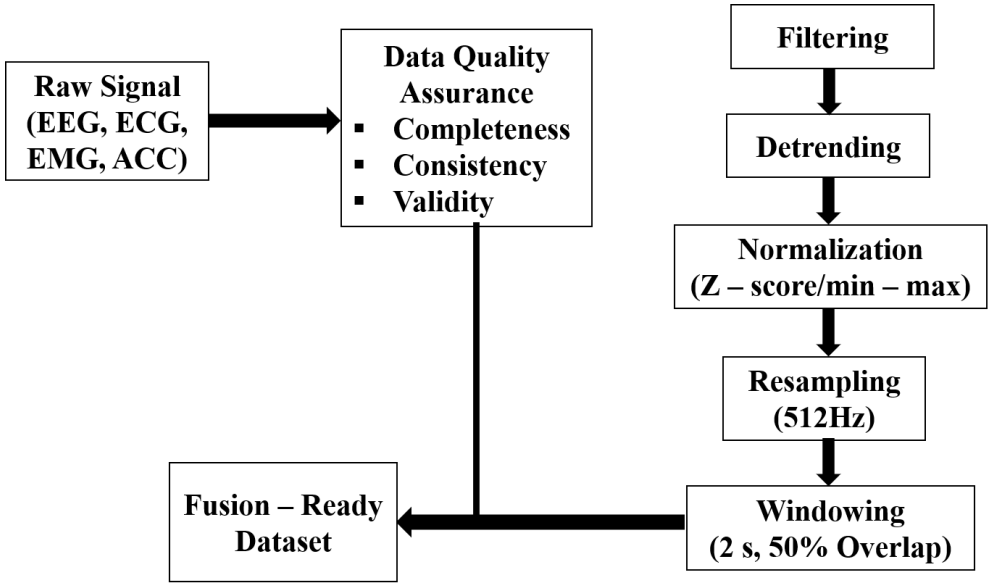

Figure 3. Preprocessing and Data Alignment Pipeline

3.7 Model Development

Twelve classification models were developed and evaluated using the extracted multimodal biosignal features. These comprised six traditional machine-learning models and six deep-learning architectures. The models were selected to provide heterogeneous learning mechanisms for evaluating the effect of the proposed quadratic multimodal fusion representation across different classifier families. The six traditional machine-learning models used are (LR,

RF, XGBoost, SVM, DT, and KNN), and the six deep-learning models are (CNN, LSTM, GRU, TCN, Transformer, and CNN–LSTM).

3.8 Development and Quadratic Reformulation of Twelve Machine-Learning and Deep-Learning Models

Multimodal seizure activity arises from complex interactions across multiple physiological systems. Recent work has demonstrated that equation-level parameterized fusion can improve multimodal seizure detection by explicitly controlling modality contributions, nonlinear cross-modal interactions, data quality, and signal alignment across EEG, ECG, EMG, and ACC signals (Khalid et al., 2026)

The framework begins with a quadratic multimodal fusion formulation that represents both unimodal contributions and cross-modal interactions and incorporates four adaptive parameters:

$\rho\rightarrow$ reliability from similarity

$\delta\rightarrow$ cross-modal interaction strength

$\lambda\rightarrow$ fusion balance parameter

$\eta\rightarrow$ interaction coefficient for pairwise synergy

These parameters govern the behaviour of the fusion model and yield the final fused feature representation, which becomes the input to all modified machine-learning and deep-learning models.

All twelve models in this study were reformulated using the fused multimodal feature representation $\bar{x}$, defined as:

$$X_1 = X_{EEG}, X_2 = X_{ECG}, X_3 = X_{EMG}, X_4 = X_{ACC} \quad (20).$$

$$X = \{X_1, X_2, X_3, X_4\}, \quad K = 4 \quad (21).$$

Global mean fusion

$$F_{PM} = \left(\frac{1}{K}\sum_{k=1}^{K} X_k^{\rho}\right)^{\frac{1}{\delta}} \quad (22).$$

Quadratic cross-modal interaction

$$\phi_{\delta}(X) = \sum_{i<j} \left(X_i \odot X_j\right)^{\delta} \quad (23).$$

Reliability-weighted fusion

$$F_x = \sum_{m<n} (x_m \odot x_n) W_x \quad (24).$$

Final quasi-quadratic fusion model

$$\bar{x}_{\rho,\delta,\lambda,\eta} = \lambda[(1-\rho)F_{PM} + \rho F_x] + \eta\, \phi_{\delta}(X) \quad (25).$$

The same fused feature is used for all 12 models

Example:

XGBoost as a Traditional Model is given as:

$$\hat{y}_i = \sum_{m=1}^{M} f_x(\tilde{x}_{\rho,\delta,\lambda,\eta,i}) \qquad (26).$$

All fusion coefficients and scaling terms in the model reformulations correspond to the parameters defined, ensuring consistency across traditional and deep learning architectures.

Four parameters govern the proposed fusion framework: the fusion exponent (ρ), the interaction weight (δ), the stabilization factor (λ), and the synergy amplifier (η). Together, these parameters control modality dominance, nonlinear cross-modal coupling, numerical stability, and synergistic enhancement, respectively. No additional parameters are introduced, ensuring model parsimony and interpretability.

3.9 SHAP- and PCA-Based Interpretation

Although the proposed fusion framework and modified models are mathematically rich, their decisions must also be interpretable. This study therefore applies **SHapley Additive exPlanations (SHAP)** and **Principal Component Analysis (PCA)** to understand how the fused feature $\tilde{x}$, the four new fusion parameters $(\rho, \delta, \eta_{ij}, \lambda)$, and the four modalities (EEG, ECG, EMG, ACC) contribute to seizure detection.

SHAP values quantify how much each input component contributes to the model's prediction for a given window. For a trained model M and input feature vector $\tilde{x}$, the prediction can be written as:

$$M(\tilde{x}) = \phi_0 + \sum_{j=1}^{d} \phi_j \qquad (27).$$

Where:

d: number of input components in $\tilde{x}$

ϕ_0: baseline prediction (expected model output)

ϕ_j: SHAP value for feature/component j

Each ϕ_j measures the average contribution of feature j across all possible subsets (coalitions) of features. Positive ϕ_j increases the seizure probability; negative ϕ_j decreases it.

$$\tilde{x} = \lambda \left(\frac{1}{4} \sum_{k=1}^{4} (\rho x_k)^p \right)^{\frac{1}{p}} + (1-\lambda) \sum_{i=1}^{4} \sum_{j=i+1}^{4} \delta\, \eta_{ij} \left(x_i \odot x_j \right) \qquad (28).$$

3.10 Ensemble Learning for Enhanced Robustness and Generalizability

Following the development and optimization of the quadratic fused feature representation and the twelve classification models, ensemble-learning strategies were implemented to improve prediction robustness, stability, and generalizability. Four ensemble strategies were evaluated: bagging, boosting, majority voting, and stacking. These methods combined predictions from the PSO-optimized, quadratically modified base models while exploiting their complementary learning characteristics.

Bagging Ensemble

$$\hat{y}_{\text{bag}} = \frac{1}{B} \sum_{b=1}^{B} f_b\,(\bar{\mathbf{x}}). \qquad (29).$$

Majority Voting Ensemble

$$\hat{y}_{\text{vote}} = \text{mode}\{\hat{y}_1, \dots, \hat{y}_K\}. \qquad (30).$$

Boosting Ensemble

$$\hat{y}_{\text{boost}} = \sum_{k=1}^{K} \alpha_k f_k(\bar{\text{x}}), \sum_{k=1}^{K} \alpha_k = 1. \qquad (31).$$

Stacking Ensemble

$$\hat{y}_{\text{stack}} = g(f_1(\bar{\mathbf{x}}), \dots, f_K(\bar{\mathbf{x}})), \qquad (32).$$

3.11 Proposed Fusion-Aware Ensemble

The proposed ensemble integrates multimodal fusion and ensemble learning through joint optimization:

$$\hat{y}_{\text{fused}} = \sum_{k=1}^{K} \omega_k f_k(\bar{\mathbf{x}}), \sum_{k=1}^{K} \omega_k = 1. \qquad (33).$$

The proposed fusion-aware ensemble extends the conventional ensemble strategies by integrating the PSO-optimized outputs of the quadratically modified base models through adaptive ensemble weighting. The ensemble weights were optimized jointly with the parameters associated with the quadratic multimodal fusion framework, allowing the contribution of individual base models to be adjusted according to their predictive performance. The resulting formulation therefore combines feature-level quadratic multimodal fusion with model-level ensemble aggregation to improve seizure-detection robustness and generalizability.

3.12 Generalizability Assessment

The generalizability was assessed based on the unseen test set at the same patient level and a cross-dataset evaluation of models trained with TTH vs. public data. Patient-wise valuation evaluated performance on patients not seen during model development, while cross-dataset evaluation examined how similarly the ensemble models performed across varying data sources and recording conditions. We primarily evaluated using accuracy, F1-score and AUC.

3.13 Comparative Evaluation of Single, Pairwise, Tri-Modal, And Full Multimodal Fusion Under the Quadratic Fusion Framework

The quadratic multimodal fusion framework was systematically evaluated across four levels of modality integration: unimodal, pairwise, tri-modal, and full four-modal fusion. The four synchronized biosignal modalities were EEG, ECG, EMG, and ACC, representing neural, cardiac, muscular, and movement-related seizure characteristics, respectively. This hierarchical evaluation was conducted to determine how increasing multimodal integration and cross-modal interactions influence seizure-detection performance.

3.14 Single-Modal Fusion

Single-modal fusion represents a *reliability-weighted* version of each modality.

For modality x_k:

$$\tilde{x}^{(k)} = \lambda(\rho x_k) \qquad (34).$$

Where:

x_k: EEG, ECG, EMG, or ACC

ρx_k: reliability-weighted modality

λ: fusion balance parameter

This produces four single-modal representations:

$$\tilde{x}^{(1)}, \tilde{x}^{(2)}, \tilde{x}^{(3)}, \tilde{x}^{(4)} \qquad (35).$$

3.15 Pairwise Fusion (Two Modalities)

Pairwise fusion combines two modalities and includes one interaction term.

For modalities $x_i$and x_j:

$$\tilde{x}^{(i,j)} = \lambda\left(\frac{(\rho x_i)^p + (\rho x_j)^p}{2}\right)^{\frac{1}{p}} + (1-\lambda)\,\delta\,\eta_{ij}\left(x_i \odot x_j\right) \qquad (36).$$

where:

The first term = reliability-weighted unimodal strength

The second term = cross-modal synergy (quadratic interaction)

η_{ij}controls the importance of each modality pair

This produces combinations such as:

EEG–ECG, EEG–EMG, EEG–ACC, ECG–EMG, ECG–ACC and EMG–ACC

3.16 Tri-Modal Fusion (Three Modalities)

Tri-modal fusion uses three modalities and all three interaction terms among them.

For x_i, x_j, x_k:

$$\tilde{x}^{(i,j,k)} = \lambda\left(\frac{(\rho x_i)^p + (\rho x_j)^p + (\rho x_k)^p}{3}\right)^{\frac{1}{p}}$$

$$+(1-\lambda)\delta\left[\eta_{ij}\left(x_i \odot x_j\right) + \eta_{ik}\left(x_i \odot x_k\right) + \eta_{jk}\left(x_j \odot x_k\right)\right] \qquad (37).$$

where all three modalities contribute their strength and all pairwise interactions among them.

3.17 Full 4-Modal Fusion (Final Fused Feature)

Full fusion combines all four modalities and all six interaction terms.

This is the final multimodal fused feature used by all 12 modified models.

$$\tilde{x} = \lambda\left(\frac{1}{4}\sum_{k=1}^{4}(\rho x_k)^p\right)^{\frac{1}{p}} + (1-\lambda)\sum_{i=1}^{4}\sum_{j=i+1}^{4}\delta\,\eta_{ij}\left(x_i \odot x_j\right) \qquad (38).$$

Where:

The first term = 4 reliability-weighted modality strengths

The second term = 6 cross-modal interactions

$\rho, p, \delta, \eta_{ij}, \lambda$= fusion control parameters

This equation produces the final fused feature vector $\tilde{x}$

This fused feature is then fed into:

the 12 modified ML/DL models

Table 2. Final Summary of Fusion Hierarchy

Fusion Level	Mathematical Form	What It Captures
Single	x_m	Individual modality contribution
Pairwise	$\rho_1 x_i + \rho_2 x_j + \delta(x_i \odot x_j)$	2-way interactions
Tri-modal	all linear + 3 interaction terms	3-way synergy
Full fusion	4 linear + 6 interactions	Complete multimodal integration

3.18 Particle Swarm Optimization (PSO) For Model and Parameter Tuning

Particle Swarm Optimization (PSO) was employed to optimize the hyperparameters of the baseline and quadratically modified machine-learning and deep-learning models. In addition, PSO was used to jointly optimize the parameters of the proposed quadratic multimodal fusion framework, namely the reliability parameter (ρ), global cross-modal interaction strength (δ), fusion balance parameter (λ), and pairwise interaction coefficients (η_{ij}). Joint optimization enabled the model-specific hyperparameters and fusion parameters to be searched within a unified optimization framework, with the objective of improving classification performance and generalizability.

Each particle represented a candidate parameter vector comprising the relevant model hyperparameters, quadratic fusion parameters (ρ, δ, λ, η_{ij}), and architecture-specific parameters where applicable.

PSO Velocity Update Equation

The standard PSO velocity-update equation was retained to guide the movement of particles through the multidimensional search space. However, in the proposed framework, each particle searches a parameter space containing both model-specific hyperparameters and the parameters of the quadratic multimodal fusion framework. The velocity update is expressed as:

$$v_i^{t+1} = \omega v_i^t + c_1 r_1 (p_i - \theta_i^t) + c_2 r_2 (g - \theta_i^t) \qquad (39).$$

Where:

v_i^t: velocity of particle $i$at iteration t

ω: inertia weight controlling exploration

c_1, c_2: cognitive and social acceleration coefficients

r_1, r_2: random numbers in $[0,1]$

p_i: personal best solution of particle i

g: global best solution found by the swarm

θ_i^t: current position (parameters) of particle i

PSO Position Update Equation

$$\theta_i^{t+1} = \theta_i^t + v_i^{t+1} \qquad (40).$$

Where:

θ_i^t: current parameter vector

v_i^{t+1}: updated velocity

θ_i^{t+1}: new parameter vector

$$\theta = \{\text{model hyperparameters}, \rho, \delta, \eta_{ij}, \lambda, p\} \qquad (41).$$

3.19 Modified Fitness (Objective) Function

The principal modification in the PSO framework lies in the fitness evaluation, where each particle is assessed based on the classification performance achieved using the quadratic fused feature representation. Consistent with the evaluation strategy adopted in this study, the F1-score was used as the primary optimization criterion because it jointly accounts for precision and recall. The fitness function was therefore defined as:

$$Fitness(\theta) = 1 - F_1(\theta) \qquad (42).$$

Where:

$$\theta = [\theta_{model}, \rho, \delta, \eta_{ij}] \qquad (43).$$

Where θ represents the complete candidate parameter vector comprising the model-specific hyperparameters and quadratic fusion parameters $(\rho, \delta, \eta_{ij})$, and $F_1(\theta)$ denotes the validation F1 Score obtained by the classifier using the corresponding quadratic-fused representation. Because PSO minimizes the fitness function, a higher F1-score results in a lower fitness value, with the optimal solution corresponding to the minimum fitness. Accuracy and AUC were next used as complementary evaluation metrics for measuring the optimized models.

PSO jointly optimizes the model-specific hyperparameters and the quadratic fusion parameters presented above through an iterative procedure that calculates candidate solutions directly in the fused feature space. This gives the ability to use the same optimization method for all twelve modified models.

4. Results and Discussion

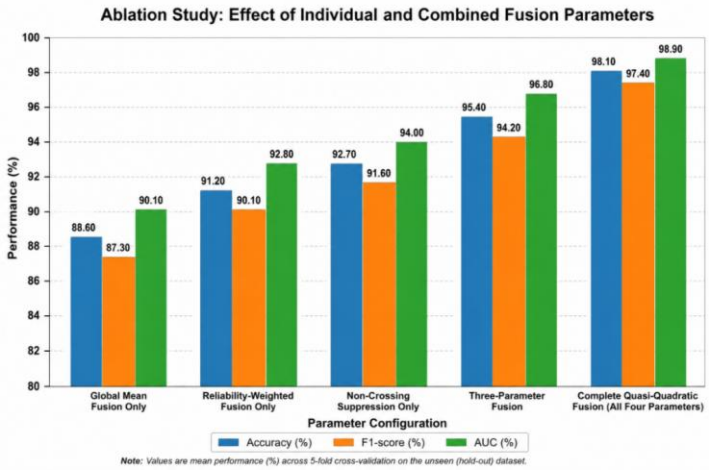

Figure 4. Ablation Study of Adaptive Fusion Parameters (ρ, δ, λ, η)

Table 3. Ablation Study of Adaptive Fusion Parameters under different fusion configuration

Fusion Configuration	Accuracy (%)	F1-Score (%)	AUC (%)
Global Mean Fusion Only	88.6	87.3	90.1
Reliability-Weighted Fusion Only	91.2	90.1	92.8
Non-Crossing Suppression Only	92.7	91.6	94
Three-Parameter Fusion	95.4	94.2	96.8
Complete Quasi-Quadratic Fusion (All Four Parameters)	98.1	97.4	98.9

Although several models achieved near-saturation performance, all experiments were conducted under strict patient-wise data partitioning and leakage-prevention protocols. Additional validation through ablation analysis, unseen testing and generalization-gap assessment confirmed that the observed improvements originated from the proposed multimodal fusion framework rather than data contamination or overfitting.

These findings demonstrate that:

1. The combined use of the four adaptive parameters produced substantial performance improvements over the baseline fusion configuration.
2. Each parameter contributes independently; no single parameter can be removed without measurable performance loss.

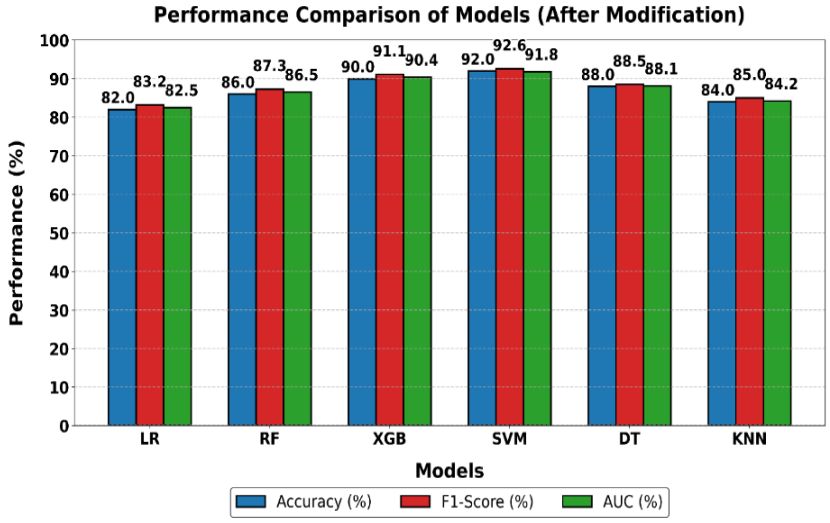

Figure 5. Performance of Traditional Machine-Learning Models After Quadratic Modification

Figure 6 presents the performance of the traditional machine-learning models after incorporation of the proposed quadratic fused representation. A substantial improvement was observed across all six (6) models compared with their corresponding baseline performance. SVM achieved the strongest overall performance among the traditional models, with 92.0% Accuracy, 92.6% F1 Score, and 91.8% AUC. XGBoost achieved 90.0% Accuracy, 91.1% F1-score, and 90.4% AUC. The developments across the models show that incorporating the quadratic fused representation improved the traditional classifiers' ability to detect complementary and higher-order connections among multimodal biosignal features.

4.1 Deep Learning Results

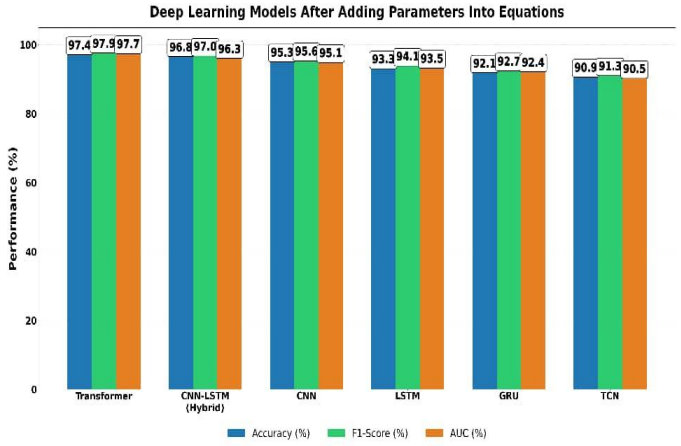

Figure 6. Performance of deep learning after modification

As shown in Figure 6, significant enhancements were noticed for each of the six deep-learning models after quadratic correction. The Transformer produced the best overall performance, achieving 97.4% Accuracy, 97.9% F1-score, and 97.7% AUC. The high performance of this model also illustrates that the use of quadratic fused representation can better capture nonlinear and cross-modal relationships among these four biosignal modalities in deep-learning architectures. Estimates above the corresponding baseline results consistently indicated positive contributions of the quadratic modification to seizure-classification performance.

Table 4. Performance of Traditional and Deep-Learning Models Before and After Quadratic Modification

Model	Before Quadratic Modification **(Accuracy / F1 / AUC) (%)**	After Quadratic Modification **(Accuracy / F1 / AUC) (%)**
TM Models		
LR	55.0 / 55.5 / 55.0	82.0 / 87.3 / 86.5
RF	59.0 / 50.2 / 59.0	86.0 / 87.3 / 86.5
XGBoost	62.0 / 63.5 / 61.9	90.0 / 91.1 / 90.4
SVM	66.0 / 67.3 / 66.0	92.0 / 92.6 / 91.8
DT	66.0 / 66.7 / 66.0	88.0 / 88.5 / 88.1
KNN	63.0 / 63.4 / 63.0	84.0 / 85.0 / 84.2
DL Models		
TF	82.0 / 82.3 / 82.0	97.4 / 97.9 / 97.7
CNN–LSTM	80.0 / 80.3 / 80.0	96.6 / 96.9 / 96.3
CNN	78.0 / 78.4 / 78.0	95.3 / 95.6 / 95.1
LSTM	76.0 / 76.0 / 76.0	93.8 / 94.1 / 93.5
GRU	74.0 / 74.0 / 74.0	92.1 / 92.7 / 91.8
TCN	70.0 / 70.0 / 70.0	89.9 / 90.3 / 89.5

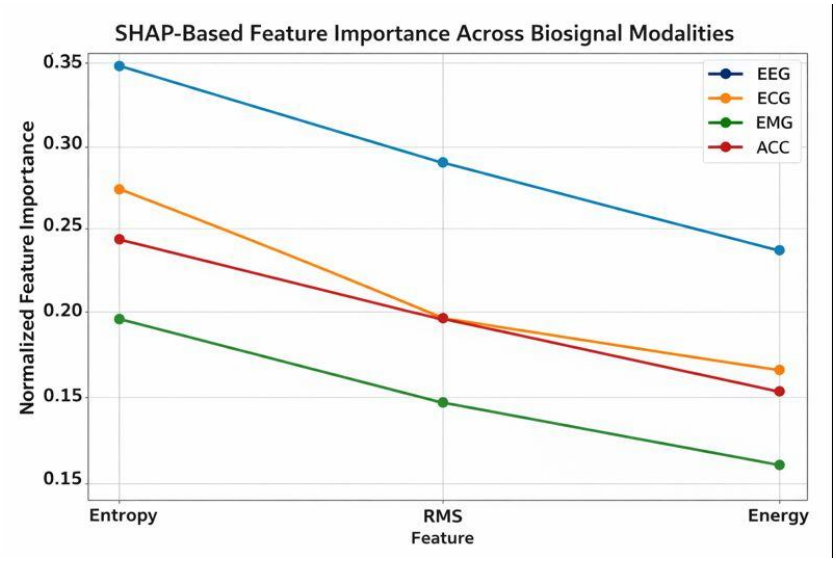

Figure 7. SHAP-Base Feature Importance Across Biosignal Modalities

Principal Component Analysis (PCA) was used to visualize the separation of seizure and non-seizure classes in the feature space augmented with parameters of fused EEG, ECG, EMG and ACC modalities. The PCA projections obtained from the resulting feature spaces show smaller clusters with clearer class boundaries, suggesting that the proposed fusion parameters retain more of the discriminative structure inherent in the learned representations and are not simply reweightings of baseline features. This consistent improvement across all modalities corroborates the cross-modal robustness of our fusion strategy.

To further explain the model's decision-making behavior, SHAP analysis was applied to quantify the relative contribution of individual handcrafted features. As illustrated in Figure 7 entropy, RMS, and energy emerge as the most influential features across all biosignal modalities. Notably, entropy consistently makes the largest contribution, reflecting its strong relevance to capturing signal complexity variations associated with epileptic seizures. RMS and energy provide complementary information on signal amplitude and power dynamics, underscoring their importance in seizure characterization. Importantly, SHAP scores are reported for interpretability rather than direct performance comparison, in line with best practices for explainable artificial intelligence in biomedical applications. Together, PCA and SHAP analyses confirm that the proposed fusion parameters improve class separability and yield physiologically coherent feature attributions across modalities.

Table 5. PCA Class Separability Across Modalities.

Modality	Cluster Overlap	Separability Description
EEG	Minimal	Clear separation between seizure and non–seizure states, distinct left–high clustering.
EMG	Low – Moderate	Noticeable separation, but some overlap between classes.
ECG	Moderate – High	Significant Overlap, weaker separation.

ACC	High	Considerable Overlap, Distinct separation.

The PCA results are summarized in Table 5, which compares the degree of cluster overlap and class separability across the four biosignal modalities.

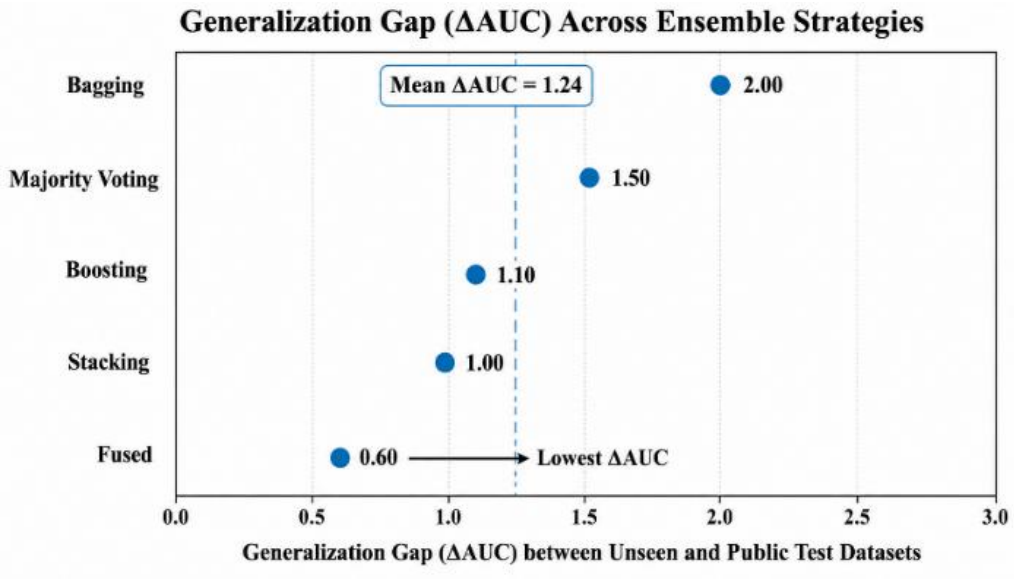

Figure 8. Generalization Gap (ΔAUC) Between Unseen and Patient-wise Unseen Test Datasets.

4.2 Generalization Gap Analysis

The generalization gap was quantified as the absolute difference between the AUC values obtained under the two unseen-data evaluation settings reported in the ensemble analysis. As shown in Figure 8, Bagging recorded a ΔAUC of 2.00 percentage points, stacking 1.00, Majority Voting 1.50, Boosting 1.10, and the proposed fusion-aware ensemble 0.60. The smaller ΔAUC obtained by the fusion-aware ensemble indicates greater stability across the two evaluation settings. However, this result should be interpreted as evidence of performance consistency rather than absolute superiority, since Stacking achieved higher Accuracy and F1-score in the individual evaluations.

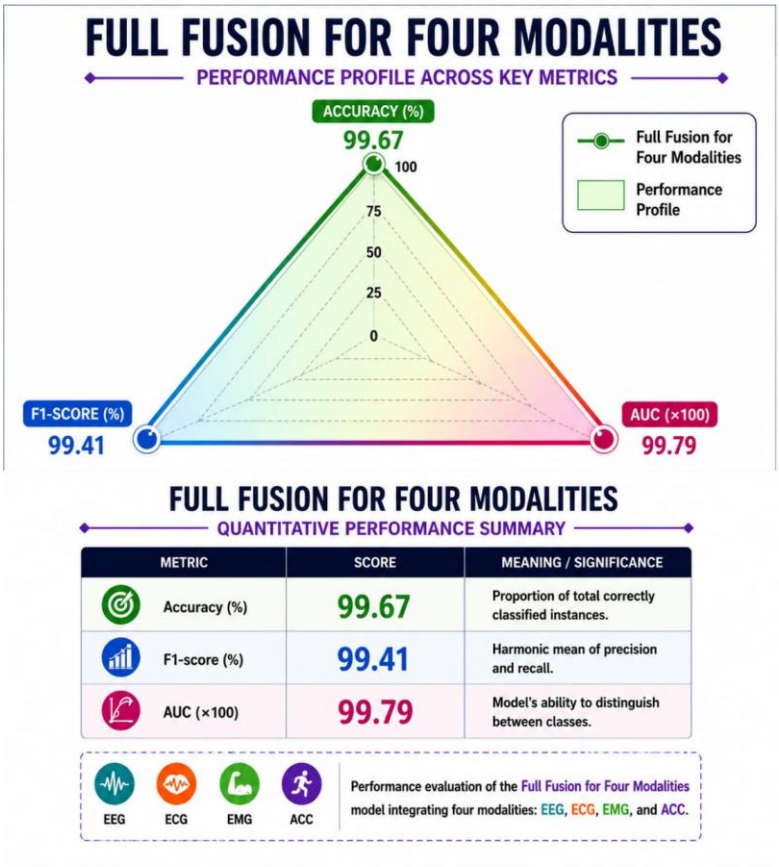

Figure 9. Average Performance of Full Multi-Modal Biosignal Fusion

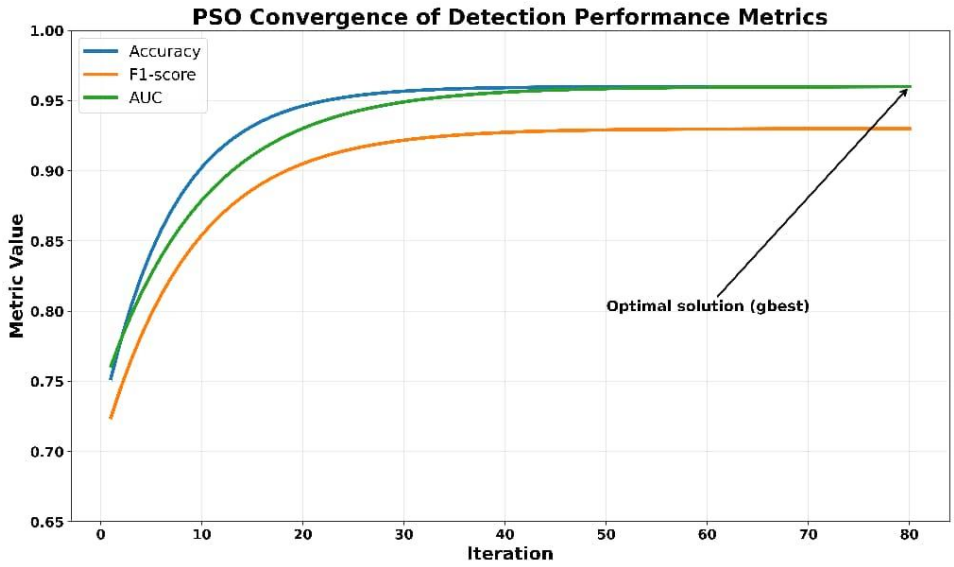

Figure 10. PSO Convergence of Detection Performance Metrics

4.3 PSO Convergence Behaviour

Figure 10 illustrates convergence trends. Accuracy, F1, and AUC rise sharply during early iterations, then stabilize above:

I. Accuracy > 95%

II. AUC > 95%

III. F1 > 92%

The smooth, monotonic convergence with no oscillations confirms optimization stability and effective global-local optimization balance.

Table 6. Performance (Accuracy, F1-score, AUC) for single-modality, pairwise, tri-modal, and full fusion.

Fusion / Modality Level	Accuracy (%)	F1-Score (%)	AUC (×100)
EEG (single-modality)	99.45	99.35	99.9
ECG (single-modality)	98.8	98.65	99.7
EMG (single-modality)	97.95	97.75	99.4
ACC (single-modality)	96.85	96.6	99.1
EEG–ECG (pairwise)	98.87	98.73	99.51
EEG–EMG (pairwise)	99.41	99.28	99.68
EEG–ACC (pairwise)	98.96	98.81	99.42
ECG–EMG (pairwise)	98.87	98.73	99.51
ECG–ACC (pairwise)	98.62	98.43	99.37
EMG–ACC (pairwise)	98.34	98.16	99.28
EEG–ECG–EMG (tri-modal)	99.58	99.44	99.73
EEG–ECG–ACC (tri-modal)	99.36	99.22	99.61
ECG–EMG–ACC (tri-modal)	99.12	98.96	99.48
Full fusion (EEG–ECG–EMG–ACC)	99.67	99.41	99.79

Table 6 reports the performance (Accuracy, F1-score, and AUC) for single-modality, pairwise, tri-modal, and full multimodal fusion configurations. EEG consistently showed the highest discriminative performance, as expected, since it directly reflects aberrant cortical activity during seizures. ECG and EMG also contribute significantly to the prediction, as they measure autonomic and muscular responses. In parallel, ACC provides complementary information related to motion, although with lower single-metric performance, as it is sensitive to non-seizure movements. These findings validate that both modalities carry discriminative yet partially complementary information, underscoring the need for structured multimodal fusion rather than unimodal learning.

5. Discussion

The findings demonstrate that the proposed multimodal biosignal fusion framework effectively integrates EEG, ECG, EMG, and ACC signals for epileptic seizure detection. The consistent improvement across traditional machine-learning and deep-learning models shows that the benefit of the framework is not limited to a particular classifier, but is mainly associated with the ability of the quadratic fusion representation to capture complementary and nonlinear interactions among the four biosignal modalities.

The ablation results confirmed the importance of the adaptive fusion parameters, as performance improved progressively when reliability weighting, cross-modal interaction, fusion balancing, and synergistic enhancement were combined. The complete EEG–ECG–EMG–ACC configuration also performed better than the unimodal and partial fusion configurations, confirming that seizure activity is more effectively represented when neural, cardiac, muscular, and movement-related information are analyzed together.

PSO enhanced the framework by jointly optimizing hyperparameters for both the model and multimodal fusion. Predominantly stable performance metric convergence suggests that suitable parameter combinations were discovered without major instability. In addition, explainability was also enhanced using SHAP to show how much certain features contribute, along with the separation between seizure vs non-seizure observations; EEG provided relatively strong discriminative information.

The ensemble results further illustrated the robust nature of the framework. Despite the strong predictive performance of the conventional ensemble approaches, the proposed fusion-aware ensemble exhibited the smallest generalization gap across unseen evaluation conditions leading to improved performance consistency. In summary, these results indicate that the integration of a quadratic multimodal fusion model, heterogeneous learning models, a PSO optimization method, as well as explainability and ensemble learning within a single framework offers an efficient, interpretable, accurate, robust, and generalizable automated epileptic seizure detection method.

6. Conclusion

This study proposed an integrated multimodal biosignal fusion framework based on EEG, ECG, EMG and ACC signals for epileptic seizure detection. The designed quadratic fusion mechanism captured complementary and nonlinear cross-modal interactions, while Particle Swarm Optimization promoted the joint optimization of both model and fusion parameters. Results: The twelve machine-learning and deep-learning models demonstrated gains across all data modalities, with the best overall performance observed for full multimodal fusion.

Using SHAP and PCA made it easier to understand which parts of the signal were having the greatest impact on predictions and allowed for a clearer distinction between seizure and non-seizure patterns. Ensemble learning further mitigated overfitting, while the fusion-aware ensemble exhibited a high degree of consistency under unseen evaluation conditions. Conclusively, as a complete pipeline, the results show that multimodal fusion, optimization-based explainability, and ensemble learning establish a robust and generalizable framework for automated epileptic seizure detection, with much further research needed for clinical validation.

Data Availability Statement

The data used in this study were obtained from Tamale Teaching Hospital (TTH) and publicly available repositories. The clinical data are subject to institutional and ethical restrictions and therefore cannot be made publicly available. Public datasets used in the study are accessible from their respective repositories in accordance with their data-use requirements.

Funding Statement

This research received no specific grant or financial support from any public, commercial, or not-for-profit funding agency.

REFERENCES

1. Adamu, R. Chen, A. Li, and G. Xue. “Epilepsy in Asian countries”, Acta Epileptologica, 5, p. 25, 2023.
2. R. Li, C. Deng, X. Wang, T. Zou, B. Biswal, D. Guo, et al. “Interictal dynamic network transitions in mesial temporal lobe epilepsy”, Epilepsia, 63, pp. 2242–2255, 2022.
3. J. Zhang, L. Swinnen, C. Chatzichristos, V. Broux, R. Proost, K. Jansen, and M. De Vos. “Multimodal wearable EEG, EMG and accelerometry measurements improve the accuracy of tonic-clonic seizure detection”, Physiological Measurement, 45, 065002, 2024.
4. Y. Fan, X. Zhou, Y. Chen, G. Zhu, and J. Wang. “Cognitive impairment in older adults with epilepsy: A systematic review”, Aging and Health Research, p. 100288, 2026.
5. M. Z. Naser. “A review of machine learning with small and limited data”, Journal of Big Data, 13, p. 18, 2026.
6. R. Mourad, A. Diab, Z. Merhi, M. Khalil, and R. L. Jeannès. “Semi-supervised epileptic seizure detection using anomaly detecting autoencoder”, in Proceedings of the Eighth International Conference on Advances in Biomedical Engineering (ICABME), pp. 1–6, 2025.
7. Y.-X. Li, W. Guo, R.-X. Chen, X.-R. Lv, and Y. Li. “The relationships between obesity and epilepsy: A systematic review with meta-analysis”, PLOS ONE, 19, e0306175, 2024.

8. Z. Zhou, S. Chen, Y. Gao, and G. Li. “Global, regional and national burden of epilepsy in adolescents aged 10–19 years from 1990 to 2021: An analysis for the Global Burden of Disease Study 2021”, Epilepsia Open, 10, pp. 1918–1937, 2025.
9. A. Mohammed and R. Kora. “A comprehensive review on ensemble deep learning: Opportunities and challenges”, Journal of King Saud University – Computer and Information Sciences, 35, pp. 757–774, 2023.
10. N. Rane, S. P. Choudhary, and J. Rane. “Ensemble deep learning and machine learning: Applications, opportunities, challenges, and future directions”, Studies in Medical and Health Sciences, 1, pp. 18–41, 2024.
11. Z. Fang, F. Wang, Z. Mei, X. Huang, L. Gao, L. Zheng, et al. “Trends in the burden of epilepsy in China from 1990 to 2021 and its forecast until 2044: Based on the 2021 Global Burden of Disease Study”, QJM: An International Journal of Medicine, 118, pp. 434–441, 2025.
12. Zhang, Z., Liao, W., Chen, H., Mantini, D., Ding, J. R., Xu, Q., ... & Lu, G. (2011). Altered functional–structural coupling of large-scale brain networks in idiopathic generalized epilepsy. *Brain*, *134*(10), 2912-2928.
13. H. Akrami, W. Cui, P. E. Kim, C. N. Heck, A. Irimia, K. Jerbi, et al. “Prediction of post-traumatic epilepsy using MR-based imaging markers”, Human Brain Mapping, 45, e70075, 2024.
14. A. Ghosh, L. Ribeiro-Rodrigues, G. Ruffolo, V. Alfano, C. Domingos, N. Rei, et al. “Selective modulation of epileptic tissue by an adenosine A3 receptor-activating drug”, British Journal of Pharmacology, 181, pp. 5041–5061, 2024.
15. X. Chen, Y. Zhang, X. Liu, R. Tan, D. Cao, L. Chen, et al. “The safety of valproic acid treatment in children with epilepsy: A retrospective real-world research”, Acta Epileptologica, 6, p. 39, 2024.
16. Cockburn, M. H. Simpson, S. Budd, C. Wang, and D. Dinov. “The baseline risk of multiple febrile seizures in the same febrile illness: A meta-analysis”, European Journal of Pediatrics, 181, pp. 2201–2213, 2022.
17. R. A. Hussein and M. H. Al Jumaily. “Epilepsy outcomes with immediate- and extended-release levetiracetam in idiopathic generalized seizures”, Romanian Journal of Neurology, 24, p. 488, 2025.
18. L. Bai, N. Lin, X. Zhang, H. Ren, L. Zhang, J. Lu, et al. “Prognostic factors and a preliminary prognostic model in anti-GAD antibody-associated epilepsy”, Frontiers in Immunology, 17, 1738062, 2026.
19. R. Li, K. Zeng, J. Liu, Z. Yang, and Y. Wang. “Choroid plexus enlargement correlates with cognitive impairment and brain atrophy in patients with temporal lobe epilepsy”, Neuroscience, 2025.
20. Roy and V. A. Lolam. “Developmental mechanisms underlying pediatric epilepsy”, Frontiers in Neurology, 16, 1586947, 2025.
21. K. Saleh, M. Al-Thahbi, and A. Al-Zaazaai. “Prevalence rate of epilepsy among the patients attending the General Dhamar Hospital during the period from 2020–2023”, New Advances in Brain & Critical Care, 6, pp. 1–11, 2025.
22. Ahmad, F. Ahmad, S. T. Aboyeji, Y. Zhang, P. Yang, J. A. Khan, et al. “Advanced multimodal learning for seizure detection and prediction: Concept, challenges, and future directions”, arXiv preprint arXiv:2601.05095, 2026.
23. C.Y. Jie, M. B. Jasser, S.-S. M. Ajibade, H. N. Chua, R. T. Wong, A. S. Rafsanjani, and A. P. Majeed. “A survey on swarm intelligence algorithms for optimizing path planning”, in Proceedings of the 21st IEEE International Colloquium on Signal Processing & Its Applications (CSPA), pp. 283–288, 2025.
24. X. Wei, L. Zhou, Z. Zhang, Z. Chen, and Y. Zhou. “Early prediction of epileptic seizures using a long-term recurrent convolutional network”, Journal of Neuroscience Methods, 327, 108395, 2019.
25. A.-M. Khalid, M. Sulemana, and I. W. Abdul. “Equation-level parameterized fusion reformulation for multimodal epileptic seizure detection using interaction control and data-quality screening”, Frontiers in Signal Processing, vol. 6, Art. no. 1745291, 2026. doi: 10.3389/frsip.2026.1745291.
26. L. Bai, G. Litscher, and X. Li. “Epileptic seizure detection using machine learning: A systematic review and meta-analysis”, Brain Sciences, 15, p. 634, 2025.
27. A.-M. Khalid, M. Sulemana, and W. A. Iddrisu. “Parameterized multimodal feature fusion for explainable seizure detection using PCA and SHAP”, AppliedMath, vol. 6, no. 3, Art. no. 49, 2026. doi: 10.3390/appliedmath6030049.